Progress on a Whole-Atmosphere Wind and Temperature Lidar

John Smith and Xinzhao Chu
Cooperative Institute for Research in Environmental Sciences
University of Colorado Boulder, Box 216 UCB, Boulder, CO 80309, USA
Lead Author e-mail address: John.A.Smith@Colorado.EDU

Abstract: We report progress on development of a "whole atmosphere" wind and temperature lidar, which pairs an Fe Doppler lidar transmitter with a Rayleigh Doppler receiver. Significant stability improvements have been made to the original receiver, allowing us to report initial sky tests for the first time. This second iteration of the Lower Atmosphere Receiver Subsystem (LARS 2) consists of a field-widened Mach-Zehnder with an optical path length difference optimized for sensitivity to Rayleigh scattering. Use of the three available frequencies of the Fe Doppler base lidar permits a bias-free estimate of the Doppler shift. Improved mounts and a secondary chamber to further limit turbulence within the cavity of the interferometer are shown to improve the long- and short-term stability. It is hoped that this receiver architecture, by providing background wind information below the Space-Atmosphere Interaction Region (SAIR), will help us to better understand the coupling between the lower atmosphere and space.

Keywords: LARS, Mach, Zehnder, DMZ, XMZ, Fe, iron, Doppler, wind, temperature, receiver, interferometer, direct, detection, hybrid, resonance, Rayleigh

1. Introduction

The dynamics of the SAIR are heavily influenced by what occurs below. For example, the wind field below the SAIR filters the spectrum of gravity waves propagating from the surface. Gravity waves that break in the MLT region play a pivotal role in the energy and momentum budget of the SAIR. Gravity waves contribute approximately 80% to the uncertainty in the energy and momentum budget of the MLT region. The SAIR is a region important to sustaining life by serving as a barrier between the Earth and space and regulating climate. In addition, the SAIR impacts many technologies that we rely upon today, like GPS/GNSS, OTH radar, and VHF communication. Also, increasingly, the stratosphere and lower mesosphere are being exploited for commercial purposes. Understanding the coupling between the lower atmospheres and SAIR through weather and climate modeling will require extensive measurements that extend throughout these regions. What we explore in this study is a method of obtaining such measurements by marrying two mature lidar techniques- resonance-fluorescence Doppler and Rayleigh-Doppler lidar.

To profile wind and temperature from 0-105+ km, we have devised a way to combine an Fe resonance Doppler lidar with a Mach-Zehnder-based Rayleigh Doppler receiver. From the Fe resonance lidar, we derive wind and temperature from 75-105 km using the resonance technique and temperature from 30-75 km with the Rayleigh lidar technique. With the Rayleigh Doppler lidar we extend the wind measurement range of the resonance lidar down from 75 km to the surface. Both techniques are used simultaneously, and non-exclusively, to offer complete coverage of the wind field in the least understood, least monitored regions of Earth's atmosphere with virtually no trade-off in either technique's measurement precision or coverage.

2. The Fe Resonance-Fluorescence Doppler Lidar

In 2007, with the advent of suitable laser technologies, the mobile Fe Doppler lidar was funded by an NSF/MRI grant to profile wind, temperature and Fe density in the upper atmosphere with unprecedented accuracy and resolution. The measurement technique employed is identical to that for Na and K resonance Doppler lidars, whereby a narrowband transmitter is tuned to three well-defined frequencies distributed about the atomic backscatter cross-section of a strong resonance line of the metal in question. Since the spectral width of the atomic cross-section is temperature-dependent by the Maxwell-Boltzmann distribution, and the frequency offset is wind-dependent by the Doppler effect, both wind and temperature can be determined by examining the range-resolved relative backscatter strength of each of the transmitted frequencies in regions where the metal is present (typically 75-105 km). Since the strong Fe resonance lines are NUV, the Fe Doppler lidar is an effective Rayleigh lidar as well.

The Fe Doppler lidar transmitter probes the Fe a5D4 - z5D4 transition at 372.0995 nm (vac.). This wavelength is generated by doubling the output of a flashlamp-pumped, Q-switched, injection seeded Alexandrite laser tuned to 744.1990 nm (vac.). The injection seeder is stabilized by monitoring the heterodyne beat between the output of the pulsed NUV light and a CW external cavity diode laser locked to a Doppler-free feature of the Fe vapor from a hollow-cathode lamp. The wing frequencies are generated by acousto-optically shifting the NIR injection seeder alternately in time by 371 MHz to the blue and to the red, corresponding to shifts of 742 MHz in the NUV.

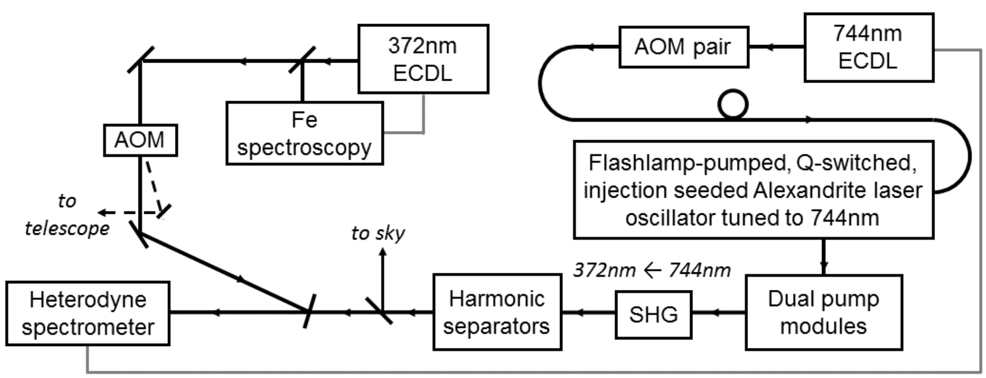

Figure1. Block diagram of MRI Fe Doppler laser transmitter system and heterodyne feedback system. Also shown is the zero-wind, CW injection AOM.

3. Lower Atmosphere Receiver Subsystem (LARS)

The LARS component is an add-on to the base Fe Doppler lidar that replaces the simple light collection receiver with a two-channel light sorting interferometer receiver. At the heart of this component is a field-widened Mach-Zehnder with an OPD of ~33 mm, optimized for sensitivity to Doppler shifts in Rayleigh backscatter of 372 nm light at stratospheric temperatures (~250 K). It is architecturally similar to the dual Mach-Zehnder, or "DMZ" design proposed and/or implemented previously [1,2], but uses the three available frequencies from the base Fe Doppler lidar to achieve a wind measurement immune from the influence of both instrumental defects and backscatter spectral width/shape, provided such modulations produce a symmetric broadening. This technique we refer to as the "XMZ" technique. A detailed description of the XMZ technique can be found in [3].

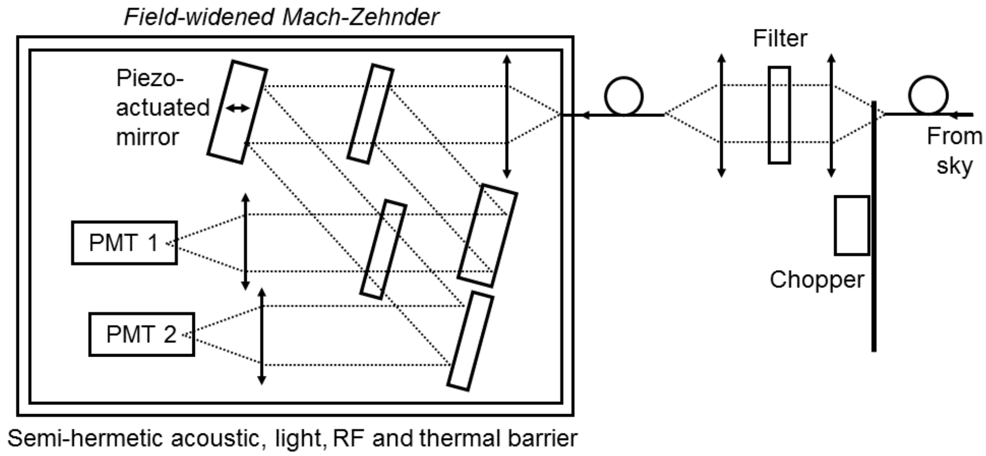

Figure 2. Sketch of the LARS 2 receiver subsystem

One leg of the interferometer is piezo-tuned to maintain the steepest slope of its sinusoidal spectral response, the cross-point of the two channels, at the zero Doppler point. In order to derive the corrections, light from the UV ECDL is "blinked" into the telescope at the end of each lidar profile to provide a zero Doppler reference. This is accomplished by a 200 MHz acousto-optic modulator, oriented to blue-shift the light, that serves as a very high-speed optical shutter. The data acquisition system sums the zero Doppler signal from both channels, then takes the difference between them and divides by their sum to derive a correction to the piezo controller.

4. Early Results and Discussion

A total of approximately 6 hours of test data were obtained at the Table Mountain Field Site 8 miles north of Boulder, Colorado between May 13th and June 13th, 2016. The 81 cm telescope was oriented to zenith to determine the zero-wind response of the receiver. A transmitter power of 1.1-1.2 W was attained using the oscillator only and the transmitter was stabilized to +80 MHz from the Fe resonance line by optical heterodyne detection and feedback. The Mach-Zehnder was stabilized to +200 MHz from the Fe resonance line by the AOM-switched light. The net shift of the MZI cross-point from the zero-wind is therefore +120 MHz.

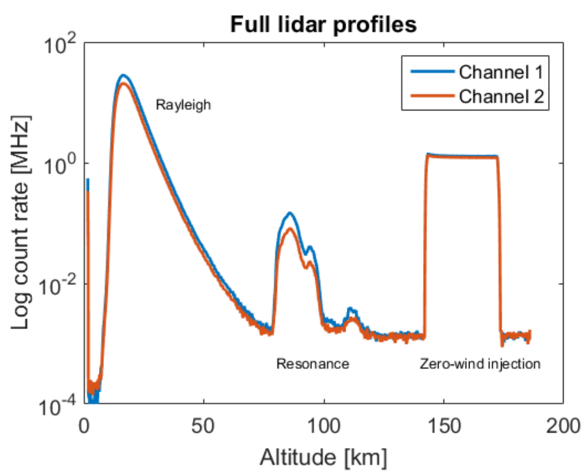

Figure 3. A full lidar profile, 30-min average, the June 13th test, un-shifted transmitter, both MZI channels, log count-rate scale, zenith direction, showing Rayleigh/Mie and resonance scattering, plus the artificial zero-wind injection near the end of the profiles.

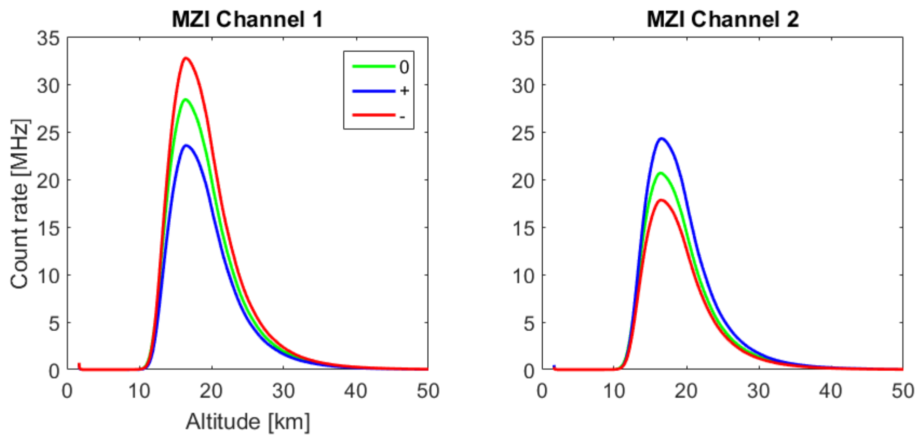

Figure 4. 30-min average lidar profiles from the same June 13th test. Un-shifted (0), blue-shifted (+) and red-shifted (-) frequencies are shown.

For each of the 3 available frequencies, we form a ratio between the difference in the channels and the sum of the channels. Defining S1, S2 and S3 as the un-shifted, blue-shifted and red-shifted signals of channel 1, respectively, and S4, S5 and S6 as the same for channel 2, the following 'Q' ratios are computed.

$$Q_1 = \frac{S_1 - S_4}{S_1 + S_4}, \quad Q_2 = \frac{S_2 - S_5}{S_2 + S_5}, \quad Q_3 = \frac{S_3 - S_6}{S_3 + S_6}$$

The Doppler shift is then, to good approximation,

$$\nu = \frac{2}{3} f_{AOM} \left(\frac{Q_1 + Q_2 + Q_3}{Q_3 - Q_2} \right) = 2\frac{v}{\lambda}$$

where f_{AOM} is the frequency between un-shifted and blue-/red-shifted profiles (+/-742 MHz). More information can be found in the literature [3]. We have discovered, in all nights of data so far, an apparent Doppler shift of approximately +500 MHz, which we have not been able to explain at this point. It could be that the interferometer is momentarily disturbed immediately following the firing of the laser in a manner that produces the observed slope in the response of the interferometer, but our preliminary tests have shown this to be a small effect. More tests are needed to identify the source of this persistent offset.

It is interesting to note that the 'Q' ratios for Rayleigh scattering are very different than the 'Q' ratios for resonance scattering due to the difference in the scattering mechanisms. Therefore, the interferometer could potentially be used as a more sensitive indicator for the presence of Fe, particularly where there is significant Rayleigh scattering contamination involved, or a high background level.

5. References

[1] Z. Liu and T. Kobayashi, "Differential Discrimination Technique for Incoherent Doppler Lidar to Measure Atmospheric Wind and Backscatter Ratio," Optical Review 3(1), 47-52 (1996).

[2] D. Bruneau, "Mach-Zehnder interferometer as a spectral analyzer for molecular Doppler wind lidar," Applied Optics 40(3), 391-399 (2001).

[3] J. Smith and X. Chu, "Investigation of a field-widened Mach-Zehnder receiver to extend Fe Doppler lidar wind measurements from the thermosphere to the ground," Applied Optics 55(6), 1366-1380 (2016).